

## Steric hindrance of ion-ion interaction in electrolytes

Emad F. Aziz, M. Freiwald, S. Eisebitt,\* and W. Eberhardt  
 BESSY m.b.H., Albert-Einstein-Strasse 15, 12489 Berlin, Germany  
 (Received 22 December 2005; published 27 February 2006)

The near-edge x-ray-absorption fine structure at the Na K-edge is compared for a solution of 1 M NaI in water vs ethanol. We find a strong influence of the solvent on the unoccupied electronic states locally at the Na<sup>+</sup> ions. The experimental data are compared to theoretical spectra based on electronic structure calculations using the density functional theory approach. The calculated spectra agree well with the experimental measurements. The comparison suggests that cation-anion interaction is important in water while it can be neglected for ethanol as a solvent. The behavior upon solvent change is rationalized by inspection of the molecular orbitals giving rise to the different spectral features.

DOI: [10.1103/PhysRevB.73.075120](https://doi.org/10.1103/PhysRevB.73.075120)

PACS number(s): 61.20.Qg, 61.10.Ht

Understanding the details of solvation processes and the interaction mechanisms within electrolytes is of wide interest for theoretical studies as well as for technological applications, such as liquid purification, homogeneous and heterogeneous catalysis, ion transport, biophysical processes, and chemical technology.<sup>1-3</sup> Despite this large importance of solvated ions, many details of the electronic structure in electrolytes, including ion-ion interaction, are poorly understood.<sup>4-6</sup> For aqueous Na<sup>+</sup> electrolytes, no evidence for ion-ion interaction was found in x-ray-diffraction studies and a surface-sensitive electron spectroscopy investigation for concentrations up to 4 M.<sup>7</sup> Recently, the near-edge x-ray-absorption fine structure (NEXAFS) at the oxygen K-edge in water has been measured with and without the presence of sodium salt.<sup>8</sup> From this experiment the authors conclude that interionic interaction between a Na<sup>+</sup> ion and the anion is negligible in up to 4 M solution. Similar results were drawn from a surface-sensitive photoemission spectroscopy study.<sup>9</sup> On the other hand, for nearly saturated or supersaturated (6.18 M) aqueous solutions of NaCl an x-ray-diffraction study reports a frequency factor of 0.3 for the occupation of a Cl<sup>-</sup> ion in direct contact [ $d(\text{Na-Cl})=2.82 \text{ \AA}$ ] with a Na<sup>+</sup> ion and an average hydration number of 4.6 for the Na<sup>+</sup> ion.<sup>10</sup> Recent EXAFS and neutron-diffraction studies on 4 and 6.4 M aqueous solutions of CaCl<sub>2</sub> report a “virtual absence” of Ca<sup>2+</sup>Cl<sup>-</sup> contact ion pairs, while a presence and an increase of *solvent-shared* ion pairs was seen on concentration increase at distances between 4.6 and 5.6 Å.<sup>11,12</sup> Molecular-dynamics (MD) studies predict a peak at 5 Å in the Na-Cl radial distribution function, with increasing coordination for increasing electrolyte concentration.<sup>13</sup> Another MD simulation predicts 25% of all ions to be included in (solvent-shared) clusters with interacting Na<sup>+</sup> and Cl<sup>-</sup> ions in 1 M solution.<sup>2</sup>

Further detailed information on the interionic interaction as well as on the influence of solvents on this interaction is thus required. In this paper, we compare Na 1 s NEXAFS spectra of 1 M NaI electrolyte with water vs ethanol as the solvent. The experimental results are compared to simulated spectra based on electronic structure calculations, carried out by density functional theory for different model clusters. The comparison of experiment and theory allows us to draw

conclusions about the Na<sup>+</sup> Cl<sup>-</sup> interaction present in the electrolytes.

NEXAFS spectroscopy is an atom selective probe of the electronic structure, with sensitivity to the modification of intra- and interatomic bond lengths and angles.<sup>14</sup> This technique has been used for studies of the gas phase as well in condensed-matter physics and chemistry.<sup>15-21</sup> For light atoms (such as C, N, or O) and shallow core levels, the relevant dipole transitions are in the soft x-ray and vacuum ultraviolet spectral range, typically requiring an evacuated experimental setup. In the last several years, such transitions have been increasingly utilized for the study of liquid materials. Topics addressed include hydrogen bond formation,<sup>8,22</sup> the molecular structure of alcohol-water mixtures<sup>22-26</sup> as well as in electrolyte solutions, and biomaterials.<sup>27,28</sup>

Because of the dipole matrix element between the Na 1 s core orbital and the unoccupied electronic states, Na 1 s NEXAFS probes the unoccupied electronic states of local *p*-symmetry in the vicinity of the Na atom. The lifetime of this electronic configuration is on the order of 1 fs. As a result, each individual absorption event is probing a frozen configuration of the atomic positions and the measurable NEXAFS spectrum is a temporal and spatial ensemble average over the different configurations. This is conceptually different to the situation encountered in spectroscopy employing longer wavelengths (such as infrared absorption), where solvent atoms will move during the interaction time. We probe the absorption via the total fluorescence yield. The experimental setup consists of a small liquid cell placed in an ultrahigh vacuum chamber. Liquid was circulated in the cell through a stainless-steel pipe under atmospheric pressure. Soft x rays were coupled into the liquid through a Si<sub>3</sub>N<sub>4</sub> membrane of 150 nm thickness. Fluorescence is detected using a GaAsP photodiode with 25 mm<sup>2</sup> active area.<sup>29</sup> Geometry-dependent saturation effects, which can be present in spectra from a concentrated specimen,<sup>21</sup> are negligible in our situation of ions diluted in a solvent. Samples were freshly prepared before the measurements. Before each measurement, the sample cell is cleaned by deionized water and a null experiment is performed, with the absence of Na 1 s absorption as a criterion for a clean sample cell. The cell is then rinsed once with the solution to be measured before the

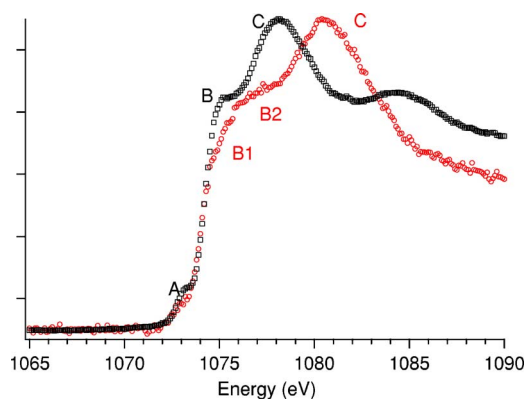


FIG. 1. (Color online) Na K-NEXAFS spectra for 1 molar solutions of NaI in water (red circles) and ethanol (black squares).

actual measurement in order to avoid uncertainties in the electrolyte concentration.

The theoretical spectra were calculated with the StoBe-deMon package<sup>30</sup> based on density-functional theory (DFT) using the standard local spin density exchange and correlation function by Vosko and Wilk.<sup>31</sup> In this calculation, effective core potentials (ECPs) with a double- $\zeta$  basis set were used for oxygen and carbon atoms of the solvent. The excited sodium ion was described using a diffused basis set, which allows a description of the core excited state and yields better results for the Rydberg and continuum states.<sup>32,33</sup> For comparison to the experiment, all calculated spectra were broadened with a Gaussian of 1.5 eV full width at half maximum (FWHM) below 1076 eV, the broadening FWHM then increases linearly to 8 eV at 1090 eV.

In Fig. 1, we present the experimental Na 1 s NEXAFS spectra for 1 M solutions of NaI in water and in ethanol. A clear difference in the NEXAFS spectra is observed, reflecting a different electronic structure locally at the Na ions, depending on the solvent. In the immediate near-edge region, three peaks can be discerned for the case of ethanol as a solvent, which we label A–C. In the case of water as a solvent, these structures are shifted to higher absorption energies as compared to the situation in ethanol. Furthermore, a shoulder develops at peak B, and we label the resulting features as B1 and B2.

We calculate the electronic structure and the resulting NEXAFS spectra by DFT using the StoBe-deMon code. In a previous concentration-dependent study for aqueous NaCl electrolytes, we have shown that  $\text{Na}^+(\text{H}_2\text{O})_6$  clusters in  $O_h$  symmetry and  $\text{Na}^+(\text{H}_2\text{O})_5\text{Cl}^-$  clusters in  $C_{2v}$  symmetry result in the best agreement of experimental NEXAFS spectra and StoBe model calculations. In particular, the experimental NEXAFS spectra for high electrolyte concentrations require  $\text{Na}^+\text{Cl}^-$  interaction as in the  $\text{Na}^+(\text{H}_2\text{O})_5\text{Cl}^-$  cluster in order to describe the experimental observations well.<sup>34</sup>

Based on these earlier results, we model the  $\text{Na}^+$  environment in solution with the following high-symmetry structures of the first hydration shell (i)  $\text{Na}^+(\text{H}_2\text{O})_5$  in trigonal bipyramidal symmetry, (ii)  $\text{Na}^+(\text{H}_2\text{O})_6$  in  $O_h$  symmetry, and (iii)  $\text{Na}^+(\text{H}_2\text{O})_5\text{I}^-$  in  $C_{2v}$  symmetry. In the case of NaI in ethanol we calculate NEXAFS spectra for a  $\text{Na}^+(\text{EtOH})_6$  cluster (with the oxygen atoms in ethanol in  $O_h$  symmetry

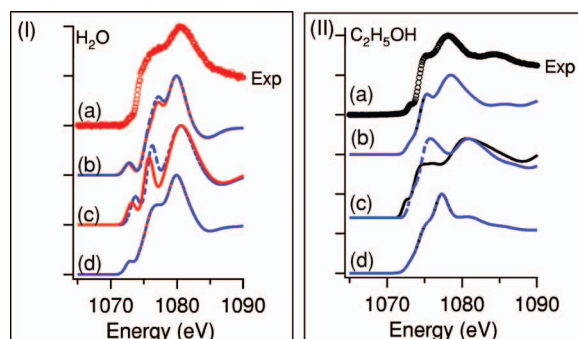


FIG. 2. (Color) Calculated Na K-NEXAFS spectra for different model clusters compared to the experimental data, shown in (a). (I) The case of  $\text{H}_2\text{O}$  as a solvent, the dashed blue line indicates results for a fixed set of bond lengths:  $d(\text{Na-O})=2.4 \text{ \AA}$  and  $d(\text{Na-I})=4.8 \text{ \AA}$ , where applicable. The red solid line indicates spectra after optimization of the bond lengths for each model as follows: (b)  $\text{Na}^+(\text{H}_2\text{O})_6$   $O_h$  symmetry with  $d(\text{Na-O})=2.42 \text{ \AA}$  (LSS=0.021), (c)  $\text{Na}^+(\text{H}_2\text{O})_5$   $T_h$  symmetry with  $d(\text{Na-O})=2.25 \text{ \AA}$  (LSS=0.031), (d)  $\text{Na}^+(\text{H}_2\text{O})_5\text{I}^-$   $C_{2v}$  symmetry with  $d(\text{Na-O})=2.4 \text{ \AA}$  and  $d(\text{Na-I})=4.8 \text{ \AA}$  (LSS=0.012). (II) The case of ethanol as a solvent, the dashed blue line indicates results for a fixed set of bond lengths,  $d(\text{Na-O})=2.47 \text{ \AA}$  and  $d(\text{Na-I})=4.8 \text{ \AA}$ , where applicable. The black solid line indicates spectra after optimization of the bond lengths for each model as follows: (b)  $\text{Na}^+(\text{EtOH})_6$  with oxygen atoms in  $O_h$  symmetry around the  $\text{Na}^+$  with  $d(\text{Na-O})=2.47 \text{ \AA}$  (LSS=0.003), (c)  $\text{Na}^+(\text{EtOH})_5$  where oxygen in  $T_h$  symmetry around  $\text{Na}^+$  with  $d(\text{Na-O})=2.3 \text{ \AA}$  (LSS=0.013), (d)  $\text{Na}^+(\text{EtOH})_5\text{I}^-$  where the oxygen atoms are in a  $C_{2v}$  symmetry around  $\text{Na}^+$  with  $d(\text{Na-O})=2.5 \text{ \AA}$  and  $d(\text{Na-I})=4.8 \text{ \AA}$  (LSS=0.020).

with respect to the  $\text{Na}^+$  ion), for  $\text{Na}^+(\text{EtOH})_5\text{I}^-$  (with the  $\text{I}^-$  ion and the oxygen atoms in ethanol in  $C_{2v}$  symmetry with respect to  $\text{Na}^+$ ), and for a  $\text{Na}^+(\text{EtOH})_5$  cluster (with the oxygen atom in the ethanol molecules in trigonal bipyramidal symmetry around the  $\text{Na}^+$  ion). In these calculations, the sodium oxygen distance  $d(\text{Na-OH}_2)$  was varied between 2.3 and 2.6  $\text{\AA}$ , which is the range indicated by x-ray diffraction,<sup>10,35</sup> and, where applicable, the sodium iodine distance  $d(\text{Na-I})$  was varied between 3.5 and 6.5  $\text{\AA}$ . To further study interionic interactions, we also calculate a  $\text{Na}^+(\text{EtOH})_6$  cluster with and without an additional  $\text{I}^-$  in the second hydration shell at 6.4  $\text{\AA}$  distance from the  $\text{Na}^+$  ion. Of course, we do realize that the situation encountered in the real electrolyte is a complex and dynamic mix of many local structures. We certainly do not want to imply that the electrolyte is made up exclusively by  $\text{Na}^+(\text{H}_2\text{O})_6$  or  $\text{Na}^+(\text{H}_2\text{O})_5\text{Cl}^-$  clusters, but we can extract useful information on the experimental data by comparison to these models by investigating trends resulting under systematic variation of the model geometry.

The calculated spectra for each cluster are presented in Fig. 2. To compare the influence of the cluster symmetry, we first calculate NEXAFS spectra for identical bond length for all symmetries, namely, with  $d(\text{Na-O})=2.40 \text{ \AA}$  for water and  $d(\text{Na-O})=2.47 \text{ \AA}$  for ethanol as a solvent. The resulting spectra are indicated by dashed lines. For both solvents, the agreement between theory and experiment seems better for the models with sixfold coordinated sodium ions than for

lower or higher coordination. To allow a more quantitative comparison between experiment and theory, the bond lengths within each model were determined by systematic variation and least-squares fitting of the calculated spectra to the experimental data. The optimum bond lengths and associated least-squares sums (LSS) are listed in the caption to Fig. 2; the resulting spectra are shown as solid lines in Fig. 2. In the case of water as a solvent, the best agreement is found between the experimental data and the calculated spectrum based on the  $\text{Na}^+(\text{H}_2\text{O})_5\text{I}^-$  model (LSS=0.012). Both the relative intensities and the peak positions of the structures A, B, and C are well reproduced. The LSS for the  $\text{Na}^+(\text{H}_2\text{O})_6$  cluster calculation (LSS=0.021) is somewhat larger than the respective value for  $\text{Na}^+(\text{H}_2\text{O})_5\text{I}^-$ , but this model does reproduce the weak splitting of peak B as observed in the experimental data. The resulting  $\text{Na}^+\text{-O}$  optimum bond length  $d(\text{Na-O})$  is 2.42 Å in the  $\text{Na}^+(\text{H}_2\text{O})_6$  model and 2.4 Å in the  $\text{Na}^+(\text{H}_2\text{O})_5\text{I}^-$  model. This range is in agreement with the cation-oxygen radial distribution function obtained by calculating the potential energy surface with respect to  $d(\text{Na}^+\text{-O})$  for the  $\text{O}_h$  cluster by a molecular-dynamics approach.<sup>36</sup> For the  $\text{Na}^+(\text{H}_2\text{O})_5\text{I}^-$  cluster, we obtain the best agreement with the experimental data for  $d(\text{Na-I})=4.8$  Å, with the first hydration shell of water around the  $\text{Na}^+$  ion located at a distance between 2.3 and 2.4 Å. The iodine ion is thus located in a distance corresponding to the second  $\text{H}_2\text{O}$  hydration shell and, together with the  $\text{Na}^+$  ion, can be regarded as a solvent-shared ion pair, similar to the situation found in the aqueous  $\text{Ca}^{2+}/\text{Cl}^-$  electrolytes.<sup>11,12</sup>

The comparison between experiment and theory for the case of ethanol as a solvent is presented in the second panel of Fig. 2. In contrast to the case of water as a solvent, the agreement of the model with pure, sixfold solvent molecule coordination to the experimental data (LSS=0.003) is significantly better than the  $\text{Na}^+(\text{EtOH})_5\text{I}^-$  model (LSS=0.020). In particular, the B/C peak intensity ratio in the  $\text{Na}^+(\text{EtOH})_5$  model calculation disagrees with the experimentally observed one and we estimate that this particular configuration cannot contribute more than 5% to the ensemble average. Calculations of NEXAFS spectra for clusters <5 or >6 ethanol molecules around a  $\text{Na}^+$  ion results in even stronger disagreement with the experimental data (not shown). In all models, the oxygen atom within the ethanol molecule is oriented toward the  $\text{Na}^+$  ion, whereas the hydrocarbon chain is pointing away from the  $\text{Na}^+$  ion; other orientations show poorer agreement to the experimental NEXAFS spectra.

As mentioned above, the best agreement between the experimental and calculated spectra is obtained in the  $\text{Na}^+(\text{EtOH})_6$  cluster model. In the  $\text{Na}^+(\text{EtOH})_5\text{I}^-$  model, we have checked radial distances  $d(\text{Na}^+\text{-O})$  from 2.3 to 2.5 Å with  $d(\text{Na}^+\text{-I}^-)$  covering the interval from 3.5 to 5.5 Å. The best agreement to the experimental data is obtained for the spectrum shown in Fig. 2(d), with a LSS that is three times larger than the spectrum based on the pure solvent model in Fig. 2(a). This finding demonstrates that  $\text{Na}^+\text{-I}^-$  interaction is much less important in the 1 M ethanol-based electrolyte as compared to the aqueous solution. The sodium oxygen distance  $d(\text{Na-O})=2.47$  Å in the  $\text{Na}^+(\text{EtOH})_6$  model is larger

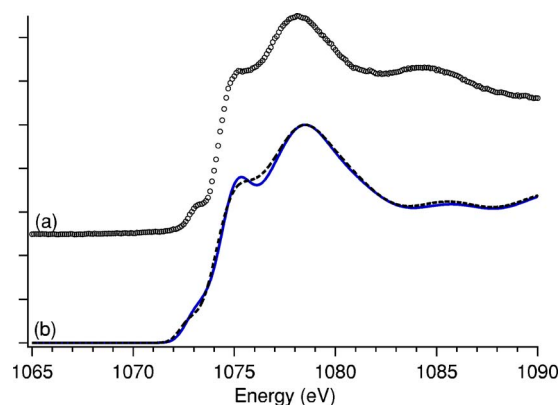


FIG. 3. (Color online) Effect of presence of the  $\text{I}^-$  anion outside of the first hydration shell on the calculated Na K-NEXAFS spectra: (a) Experimental NEXAFS for 1 M NaI in ethanol and (b) Calculated spectra for a  $\text{Na}^+(\text{EtOH})_6$  cluster (solid blue line) and a  $\text{Na}^+(\text{EtOH})_6\text{I}^-$  cluster (dashed black line) with  $d(\text{Na-I})=6.4$  Å and  $d(\text{Na-O})=2.47$  Å in both cases.

than in the equivalent water structure, which seems reasonable due to the lower amount of partial charge on the oxygen atom in the ethanol molecule as compared to water. In addition, steric interaction of the larger ethanol molecules may lead to an increase of  $d(\text{Na-O})$  in the first hydration shell as compared to the case of water as a solvent.

For the model structures tested, we are able to obtain better agreement between experiment and theory for the case of ethanol as a solvent as compared to water as a solvent. Given the smaller size of the water molecule compared to ethanol, we expect that the inclusion of a second coordination shell in the models is more important in the water case. Although we anticipate that the discrepancy between experiment and theory can be reduced, in particular, for the water case by modeling more than one hydration shell, the associated calculation of the electronic structure and the NEXAFS spectrum becomes very complex and is outside the scope of this paper.

For larger interionic distances in the  $\text{Na}^+(\text{EtOH})_5\text{I}^-$  model, we have tested the influence of interionic interaction by placing the  $\text{I}^-$  outside a  $\text{Na}^+(\text{EtOH})_6$  cluster, i.e., where the sodium ion is surrounded by a “complete” EtOH coordination shell. As shown in Fig. 3, we only observe very small changes in the calculated spectral shape (LSS=0.0030 vs 0.0028) at such interionic distances. In combination with our results presented in the context of Fig. 2, we thus conclude that ethanol efficiently excludes  $\text{I}^-$  ions from the first hydration shell at 1 M concentration. Note that in the water case, we obtain the best agreement within the  $\text{Na}^+(\text{H}_2\text{O})_5\text{I}^-$  model for  $d(\text{Na-I})=4.8$  Å. At this distance, one can expect the steric hindrance by water molecules to be small compared to the situation encountered in ethanol.

Keeping in mind that we are probing a spatial and temporal ensemble average, this different behavior in the two solvents should be reflected in the respective residence times of solvent molecules. We are not aware of a molecular-dynamics calculation comparing water and ethanol. For water vs methanol a molecular-dynamics (MD) calculation pre-



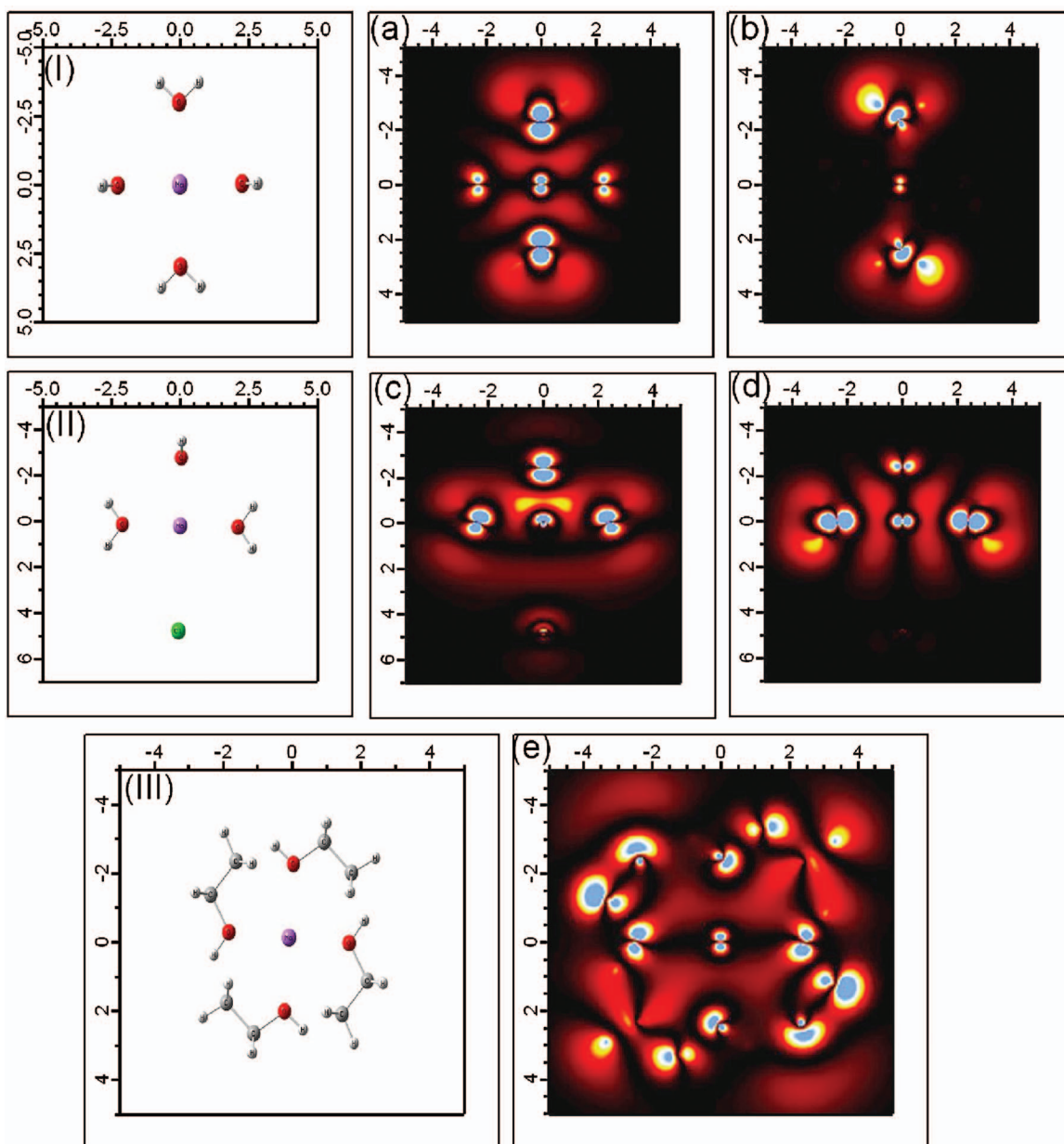


FIG. 4. (Color) Orbitals contributing to the unoccupied states giving rise to peak B. Shown in (a) and (b) are representative orbitals of the  $\text{Na}^+(\text{H}_2\text{O})_6$  cluster contributing to peaks B1 and B2, respectively. Shown in (c) and (d) are representative orbitals of the  $\text{Na}^+(\text{H}_2\text{O})_5\text{I}^-$  cluster contributing to peaks B1 and B2, respectively. (e) Representative orbital of the  $\text{Na}^+(\text{EtOH})_6$  cluster contributing to peak B. Models are shown in a plane (molecules above and below are not shown); electron density is shown for the same plane. Lateral distances are in units of Å.

dicts about half the residence time for methanol as compared to water.<sup>36</sup> If we assume similar residence time for methanol and ethanol (which both carry one OH functional group), our experimental results regarding  $d(\text{Na}-\text{O})$  exhibit a trend that is in agreement with the theoretical predictions for the HOH/MeOH case.

Finally, we want to rationalize the existence of a double structure in peak B in the case of water as a solvent, which is absent in the respective ethanol spectra. To this end, we analyze the electronic structure in the  $\text{Na}^+(\text{H}_2\text{O})_6$  model, which does exhibit the double-peak structure, and compare it to the  $\text{Na}^+(\text{EtOH})_6$  situation. Inspecting the electronic wave func-

tions, we find that two different types of orbitals give rise to the double structure in the water case. Two representative wave functions are visualized in the first panel of Fig. 4. With respect to the oxygen atom in the water molecule, they exhibit  $a_1$  vs  $b_2$  symmetry. In contrast, only one type of orbital ( $a'$  symmetry) contributes to peak B in the case of ethanol as a solvent. For completeness, we also show the respective orbitals for the  $\text{Na}^+(\text{H}_2\text{O})_5\text{I}^-$  model. The presence of the  $\text{I}^-$  ion does not change the general picture: again, two types of orbitals ( $b_1, b_2$ ) are present; the energy separation, however, is reduced compared to the  $\text{Na}^+(\text{H}_2\text{O})_6$  case and a

splitting is therefore not noticeable given the amount of broadening in the spectra.

In conclusion, we have presented experimental Na 1s NEXAFS spectra of 1 M solution of NaI in water and ethanol. Clear solvent-dependent differences in the local electronic structure are observed. The experimental data are compared to calculated spectra based on DFT calculations, including the effect of the core hole on the NEXAFS spectra. For the ethanol-based electrolyte, we find that the observed NEXAFS structure is very well modeled by a  $\text{Na}^+(\text{EtOH})_6$  cluster. Inclusion of an iodine ion in the first hydration shell leads to significant disagreement of the calculated and ex-

perimental spectra. We conclude that an anion residing in the first hydration shell of the sodium ion contributes only negligibly to the ensemble of structures encountered in the ethanol-based electrolyte. We suggest that this “exclusion” from the first hydration shell is due to steric hindrance by the solvent molecules. This situation is different in the water-based NaI electrolyte, where the comparison of experiment and theory suggests that both  $\text{Na}^+(\text{H}_2\text{O})_6$  and  $\text{Na}^+(\text{H}_2\text{O})_5\text{I}^-$  contribute significantly to the ensemble average, indicating the importance of  $\text{Na}^+\text{-I}^-$  interaction, in particular, at elevated concentrations of 1 M and above.

\*Corresponding author. Electronic address: eisebitt@bessy.de

<sup>1</sup>P. Bopp, in *The Physics and Chemistry of Aqueous Ionic Solutions*, edited by M.-C. Bellissent, and G. W. Neilson, NATO ASI Series C (Springer, Berlin, 1987).

<sup>2</sup>L. Degreve and F. L. B. da Silva, *J. Chem. Phys.* **111**, 5150 (1999).

<sup>3</sup>J. Yu, L. Degreve, and M. LozadaCassou, *Phys. Rev. Lett.* **79**, 3656 (1997).

<sup>4</sup>M. F. Kropman and H. J. Bakker, *J. Chem. Phys.* **115**, 8942 (2001).

<sup>5</sup>M. A. Carignano, G. Karlstrom, and P. Linse, *J. Phys. Chem. B* **101**, 1142 (1997).

<sup>6</sup>D. E. Smith and L. X. Dang, *J. Chem. Phys.* **100**, 3757 (1994).

<sup>7</sup>K. R. Wilson, B. S. Rude, T. Catalano, R. D. Schaller, J. G. Tobin, D. T. Co, and R. J. Saykally, *J. Phys. Chem. B* **105**, 3346 (2001).

<sup>8</sup>C. D. Cappa, J. D. Smith, K. R. Wilson, B. M. Messer, M. K. Gilles, R. C. Cohen, and R. J. Saykally, *J. Phys. Chem. B* **109**, 7046 (2005).

<sup>9</sup>R. Weber, B. Winter, P. M. Schmidt, W. Widdra, I. V. Hertel, M. Dittmar, and M. Faubel, *J. Phys. Chem. B* **108**, 4729 (2004).

<sup>10</sup>H. Ohtaki and N. Fukushima, *J. Solution Chem.* **21**, 23 (1992).

<sup>11</sup>J. L. Fulton, S. M. Heald, Y. S. Badyal, and J. M. Simonson, *J. Phys. Chem. A* **107**, 4688 (2003).

<sup>12</sup>Y. S. Badyal, A. C. Barnes, G. J. Cuello, and J. M. Simonson, *J. Phys. Chem. A* **108**, 11819 (2004).

<sup>13</sup>J. P. Brodholt, *Chem. Geol.* **151**, 11 (1998).

<sup>14</sup>J. Stöhr, *NEXAFS Spectroscopy* (Springer-Verlag, Berlin, 1992).

<sup>15</sup>Y. Okamoto, H. Shiwaku, T. Yaita, S. Suzuki, K. Minato, and H. Tanida, *Z. Naturforsch., A: Phys. Sci.* **59**, 819 (2004).

<sup>16</sup>Y. Okamoto, *Nucl. Instrum. Methods Phys. Res. A* **526**, 572 (2004).

<sup>17</sup>Y. Okamoto, Y. Iwadate, K. Fukushima, H. Matsuura, and K. Minato, *J. Phys. Chem. Solids* **66**, 452 (2005).

<sup>18</sup>A. Zimina, S. Eisebitt, M. Freiwald, S. Cramm, W. Eberhardt, A. Mrzel, and D. Mihailovic, *Nano Lett.* **4**, 1749 (2004).

<sup>19</sup>B. J. Ruck, A. Koo, U. D. Lanke, F. Budde, H. J. Trodahl, G. V. M. Williams, A. Bittar, J. B. Metson, E. Nodwell, T. Tiedje, A. Zimina, and S. Eisebitt, *J. Appl. Phys.* **96**, 3571 (2004).

<sup>20</sup>S. Eisebitt, J. E. Rubensson, T. Boske, and W. Eberhardt, *Phys. Rev. B* **48**, 17388 (1993).

<sup>21</sup>S. Eisebitt, T. Boske, J. E. Rubensson, and W. Eberhardt, *Phys. Rev. B* **47**, 14103 (1993).

<sup>22</sup>P. Wernet, D. Nordlund, U. Bergmann, M. Cavalleri, M. Odelius, H. Ogasawara, L. A. Naslund, T. K. Hirsch, L. Ojamae, P. Glatzel, L. G. M. Pettersson, and A. Nilsson, *Science* **304**, 995 (2004).

<sup>23</sup>J. H. Guo, A. Augustsson, S. Kashtanov, D. Spangberg, J. Nordgren, K. Hermansson, Y. Luo, and A. Augustsson, *J. Electron Spectrosc. Relat. Phenom.* **144-147**, 287 (2005).

<sup>24</sup>J. H. Guo, Y. Luo, A. Augustsson, S. Kashtanov, J. E. Rubensson, D. Shuh, V. Zhuang, P. Ross, H. Agren, and J. Nordgren, *J. Electron Spectrosc. Relat. Phenom.*, **137-40**, 425 (2004).

<sup>25</sup>M. Cavalleri, H. Ogasawara, L. G. M. Pettersson, and A. Nilsson, *Chem. Phys. Lett.* **364**, 363 (2002).

<sup>26</sup>J. H. Guo, Y. Luo, A. Augustsson, S. Kashtanov, J. E. Rubensson, D. K. Shuh, H. Agren, and J. Nordgren, *Phys. Rev. Lett.* **91**, 157401 (2003).

<sup>27</sup>B. M. Messer, C. D. Cappa, J. D. Smith, K. R. Wilson, M. K. Gilles, R. C. Cohen, and R. J. Saykally, *J. Phys. Chem. B* **109**, 5375 (2005).

<sup>28</sup>E. F. Aziz, A. Zimina, M. Freiwald, W. Eberhardt, and S. Eisebitt, (to be published).

<sup>29</sup>M. Freiwald, S. Cramm, W. Eberhardt, and S. Eisebitt, *J. Electron Spectrosc. Relat. Phenom.* **137-40**, 413 (2004).

<sup>30</sup>K. Hermann, L. G. M. Pettersson, M. E. Casida, C. Daul, A. Goursot, A. Koester, E. Proynov, A. St-Amant, D. R. Salahub, V. Carravetta, H. Duarte, N. Godbout, J. Guan, C. Jamorski, M. Leboeuf, V. Malkin, M. Nyberg, L. Pedocchi, F. Sim, L. Triguero, and A. Vela, StoBe-deMon Software, 2002.

<sup>31</sup>S. H. Vosko and L. Wilk, *Phys. Rev. B* **22**, 3812 (1980).

<sup>32</sup>L. Triguero, L. G. M. Pettersson, and H. Agren, *Phys. Rev. B* **58**, 8097 (1998).

<sup>33</sup>H. Agren, V. Carravetta, O. Vahtras, and L. G. M. Pettersson, *Chem. Phys. Lett.* **222**, 75 (1994).

<sup>34</sup>Structures tested: (i)  $\text{Na}^+(\text{H}_2\text{O})_4$  with Th symmetry, (ii)  $\text{Na}^+(\text{H}_2\text{O})_5$  in trigonal bipyramidal symmetry, (iii)  $\text{Na}^+(\text{H}_2\text{O})_4\text{Cl}^-$  with one  $\text{Cl}^-$  replacing an out of plane water molecule in  $\text{Na}^+(\text{H}_2\text{O})_5$ , (iv)  $\text{Na}^+(\text{H}_2\text{O})_6$  in  $O_h$  symmetry, (v)  $\text{Na}^+(\text{H}_2\text{O})_5\text{Cl}^-$  in  $C_{2v}$  symmetry, (vi)  $\text{Na}^+(\text{H}_2\text{O})_7$ , with a systematic variation of bond length and including small angle distortions of the high symmetry configurations.

<sup>35</sup>H. Ohtaki and T. Radnai, *Chem. Rev. (Washington, D.C.)* **93**, 1157 (1993).

<sup>36</sup>E. Hawlicka and D. Swiatla-Wojcik, *J. Phys. Chem. A* **106**, 1336 (2002).